β-globin gene transfer to human bone marrow for sickle cell disease

Zulema Romero,[1] Fabrizia Urbinati,[1] Sabine Geiger,[1] Aaron R. Cooper,[2] Jennifer Wherley,[1] Michael L. Kaufman,[1] Roger P. Hollis,[1] Rafael Ruiz de Assin,[1] Shantha Senadheera,[1] Arineh Sahagian,[1] Xiangyang Jin,[1] Alyse Gellis,[1] Xiaoyan Wang,[3] David Gjertson,[4] Satiro DeOliveira,[5] Pamela Kempert,[5] Sally Shupien,[5] Hisham Abdel-Azim,[6] Mark C. Walters,[7] Herbert J. Meiselman,[8] Rosalinda B. Wenby,[8] Theresa Gruber,[9] Victor Marder,[9] Thomas D. Coates,[10] and Donald B. Kohn[1,5]

[1]Department of Microbiology, Immunology and Molecular Genetics, [2]Molecular Biology Interdepartmental Ph.D. Program, [3]Department of Medicine Statistics Core, [4]Department of Biostatistics, School of Public Health, and [5]Division of Pediatric Hematology/Oncology, Department of Pediatrics, UCLA, Los Angeles, California, USA. [6]Division of Research Immunology/Bone Marrow Transplantation, Department of Pediatrics, Childrens Hospital Los Angeles, University of Southern California Keck School of Medicine, Los Angeles, California, USA. [7]Children's Hospital and Research Center, Oakland, California, USA. [8]Department of Physiology and Biophysics, University of Southern California Keck School of Medicine, Los Angeles, California, USA. [9]Division of Hematology and Medical Oncology, Department of Medicine, UCLA, Los Angeles, California, USA. [10]Division of Hematology/Oncology, Department of Pediatrics, Childrens Hospital Los Angeles, University of Southern California Keck School of Medicine, Los Angeles, California, USA.

Autologous hematopoietic stem cell gene therapy is an approach to treating sickle cell disease (SCD) patients that may result in lower morbidity than allogeneic transplantation. We examined the potential of a lentiviral vector (LV) (CCL-βAS3-FB) encoding a human hemoglobin (*HBB*) gene engineered to impede sickle hemoglobin polymerization (*HBBAS3*) to transduce human BM CD34+ cells from SCD donors and prevent sickling of red blood cells produced by in vitro differentiation. The CCL-βAS3-FB LV transduced BM CD34+ cells from either healthy or SCD donors at similar levels, based on quantitative PCR and colony-forming unit progenitor analysis. Consistent expression of *HBBAS3* mRNA and HbAS3 protein compromised a fourth of the total β-globin–like transcripts and hemoglobin (Hb) tetramers. Upon deoxygenation, a lower percentage of *HBBAS3*-transduced red blood cells exhibited sickling compared with mock-transduced cells from sickle donors. Transduced BM CD34+ cells were transplanted into immunodeficient mice, and the human cells recovered after 2–3 months were cultured for erythroid differentiation, which showed levels of *HBBAS3* mRNA similar to those seen in the CD34+ cells that were directly differentiated in vitro. These results demonstrate that the CCL-βAS3-FB LV is capable of efficient transfer and consistent expression of an effective anti-sickling β-globin gene in human SCD BM CD34+ progenitor cells, improving physiologic parameters of the resulting red blood cells.

Introduction

Sickle cell disease (SCD) is one of the most common monogenic disorders worldwide and is a major cause of morbidity and early mortality (1). Although SCD is well characterized, there is still no ideal long-term treatment. Current therapies are based on induction of fetal hemoglobin (HbF) to inhibit polymerization of sickle hemoglobin (HbS) (2) and cell dehydration (3) or reduction of the percentage of HbS by transfusions (4). Allogeneic HSC transplantation (HSCT) from BM or umbilical cord blood (UCB) is a potentially curative therapy, although only a small percentage of patients have undergone this procedure, mostly children with severe symptoms who had HLA-matched sibling donors (5–7). Transplantation of allogeneic cells carries the risk of graft-versus-host disease (GvHD), which can be a cause of extensive morbidity. HSCT using UCB from matched unrelated donors holds reduced risk of acute or chronic GvHD compared with using BM; however, there is a higher probability of engraftment failure using UCB as a result of its lower cell dose and immunologic immaturity (8, 9).

Gene therapy with autologous HSCs is an alternative to allogeneic HSCT, since it avoids the limitations of finding a matched donor and the risks of GvHD and graft rejection. For gene therapy application in SCD patients, the safest source for autologous HSC would be BM, due to the complications previously described when G-CSF was used to collect autologous peripheral blood stem cells (PBSCs) in SCD patients (10–12). Although general anesthesia imposes a risk for SCD patients as well, current best medical practices can minimize these (13).

The development of integrating vectors for β-globin gene transfer has been challenging due to the complex regulatory elements needed for high-level, erythroid-specific expression (14). γ-Retroviral vectors were unable to transfer these β-globin expression cassettes intact (15, 16); in contrast, lentiviral vectors (LV) can transfer β-globin cassettes intact with relatively high efficiency, although the titers of these vectors are reduced compared with those of vectors bearing simpler cassettes (17, 18). In the last decade, many groups have developed different β-globin LV for targeting β-hemoglobinopathies, with successful therapeutic results following transplantation of ex vivo–modified HSC in mouse models (17–23).

Sickle patients with hereditary persistence of HbF (HPFH) have improved survival and amelioration of clinical symptoms, with maximal clinical benefits observed when the HbF is elevated above threshold values (e.g., 8%–15% of the total cellular Hb) (2, 24). Therefore, some gene therapy strategies have employed viral vectors carrying the human γ-globin gene (*HBG1/2*). However, these constructs expressed HbF poorly in adult erythroid cells,

since fetal-specific transcription factors are required for high-level expression of the γ-globin gene (25, 26). These limitations have been overcome by embedding the exons encoding human γ-globin within the human β-globin gene 5′ promoter and 3′ enhancer elements (20, 27, 28). Breda et al. (29) used an LV vector encoding the human hemoglobin (HBB) gene to increase the expression of normal HbA in CD34^{+}-derived erythroid cells from SCD patients; however, the expression level needed when the HBB gene is used would be higher than would be required for HBG1/2 gene expression to achieve therapeutic benefits in SCD patients.

Another approach is to modify β-globin genes to confer anti-sickling activity by substituting key amino acids from γ-globin; the modified β-globin cassette should yield the necessary high-level, erythroid-specific expression in adult erythroid cells. Pawliuk et al. (18) designed an LV carrying a human β-globin gene with the amino acid modification T87Q; the glutamine at position 87 of γ-globin has been implicated in the anti-sickling activity of HbF (30). This anti-sickling construct corrected SCD in 2 murine models of the disease, and a similar LV has been used in a clinical trial for β-thalassemia and SCD in France (31).

Townes and colleagues have taken a similar approach, developing a recombinant human anti-sickling β-globin gene (HBBAS3) encoding a β-globin protein (HbAS3) that has 3 amino substitutions compared with the original (HbA): T87Q for blocking the lateral contact with the canonical Val 6 of HbS, E22A to disrupt axial contacts (32) and G16D, which confers a competitive advantage over sickle–β-globin chains for interaction with the α-globin polypeptide. Functional analysis of the purified HbAS3 protein demonstrated that this recombinant protein had potent activity to inhibit HbS tetramer polymerization (33). Levasseur et al. (19) showed efficient transduction of BM stem cells from a murine model of SCD with a self-inactivating (SIN) LV carrying the HBBAS3 transgene that resulted in normalized rbc physiology and prevented the pathological manifestations of SCD.

The goal of this study was to characterize the capacity of a β-AS3 LV (CCL-βAS3-FB) to transduce human BM-derived CD34^{+} cells from SCD donors for potential use in a clinical trial of gene therapy for SCD. This vector achieved efficient transduction of BM CD34^{+} cells from healthy or SCD donors. To assess the erythroid-specific expression of the HBBAS3 gene and its anti-sickling properties, we used an in vitro model of erythroid differentiation to produce mature erythroid cells from human BM CD34^{+} cells (34). We assessed the gene expression activity of the CCL-βAS3-FB at the mRNA and protein levels, characterized the effects of HBBAS3 expression on sickling of deoxygenated rbc, and performed an in vitro assay to detect potential genotoxicity. Transduced BM CD34^{+} cells were also xenografted into immunodeficient mice, and human hematopoietic progenitor cells were reisolated from the marrow of the mice after 2 to 3 months, subjected to in vitro erythroid differentiation, and found to continue to express the anti-sickling HBBAS3 gene. These results demonstrate the capability of the CCL-βAS3-FB LV to efficiently transduce SCD BM CD34^{+} progenitor cells and produce sufficient levels of an anti-sickling Hb protein to improve the physiological parameters of the rbc that may be applied for clinical gene therapy of SCD.

Results

The CCL-βAS3-FB LV vector carrying the HBBAS3 cassette. The original LV produced by Levasseur et al. (19) to carry the HBBAS3 cassette (DL-βAS3) contained the intact HIV 5′ LTR, which engenders

dependence on the HIV TAT protein for production of high-titer vector. To eliminate the need for TAT during packaging, we moved the HBBAS3 cassette plus the woodchuck hepatitis virus posttranscriptional regulatory element (WPRE) to the pCCL LV backbone (35), which is a SIN vector with the CMV enhancer/promoter substituted in the 5′ LTR, eliminating the need for TAT. This pCCL backbone was further modified to have a compact (77 bp) insulator in the U3 region of the 3′ LTR, denominated FB, which contains the minimal CTCF binding site (FII) of the 250-bp core of the 1.2-kb chicken β-globin HS4 (cHS4) insulator and the analogous region of the human T cell receptor δ/α BEAD-1 insulator (36). The resulting SIN-LV was named CCL-βAS3-FB, and the proviral form is shown in Figure 1A.

In 3 independent experiments, we packaged preparations of the CCL-βAS3-FB vector as well as a version lacking the FB insulator (CCL-βAS3), the parental DL-βAS3 vector, and a vector expressing the enhanced GFP (CCL-MND-GFP) as a positive control. The vector preparations were made with and without inclusion of a plasmid that expressed the HIV-1 TAT protein. The titers were determined by transducing a permissive cell line (HT29 human colon carcinoma) and measuring vector copies (VC)/cell using quantitative PCR (qPCR) with primers to the HIV packaging signal (Psi) of the vector proviruses (ref. 37 and Supplemental Figure 1; supplemental material available online with this article; doi:10.1172/JCI67930DS1). The CCL-βAS3-FB vector as well as the noninsulated version could be produced in the absence of TAT to a 10-fold higher titer than the original DL-βAS3 vector ($P = 0.017$, 2-tailed t test; CCL-βAS3 and CCL-βAS3-FB combined compared with the DL-βAS3), and inclusion of the FB insulator did not decrease vector titer.

The stability of the FB insulator was evaluated by PCR analysis of the FB-containing fragment size in bulk populations of transduced BM CD34^{+} cells (Figure 1B) and at a clonal level (a total of 32 single CFU colonies; data not shown). All samples showed the expected sizes of single bands after PCR analysis, demonstrating intact passage of the FB insulator. Additionally, Southern blot analysis of CCL-βAS3-FB–transduced cells showed the presence of a single band of the size expected for full-length vector provirus (Supplemental Figure 2).

To evaluate the functional activity of the FB insulator, binding of the CTCF protein to the LTRs of the CCL-βAS3-FB was assessed by ChIP in transduced K562 cells (Figure 1C). ChIP indicated a 12-fold enrichment of CTCF binding in the CCL-βAS3-FB LTR when compared with the input control; no enrichment was found with the CCL-βAS3 vector lacking the FB insulator, indicating the specific binding of the CTCF to the FB sequence. The association with CTCF to the CCL-βAS3-FB LTR was at least as high as with other sequences known to bind CTCF, such as the 1.2-kb cHS4 insulator (38), the c-Myc promoter (39), or the H19 imprinting control region (40).

Assessment of transduction and hematopoietic potential of BM CD34^{+} cells. Preliminary dose-response experiments were performed to determine the most efficient concentration of the CCL-βAS3-FB vector to transduce human BM CD34^{+} cells, using a range of vector concentrations during transduction from 2×10^6 to 2×10^8 transduction units/ml (TU/ml) (MOI = 4–400). A dose-related increase in gene transfer achieved (the average VC/cell measured by qPCR) was found only for vector concentrations below 2×10^7 TU/ml. Higher vector concentrations did not increase the transduction efficacy and, in fact, often had a negative effect on
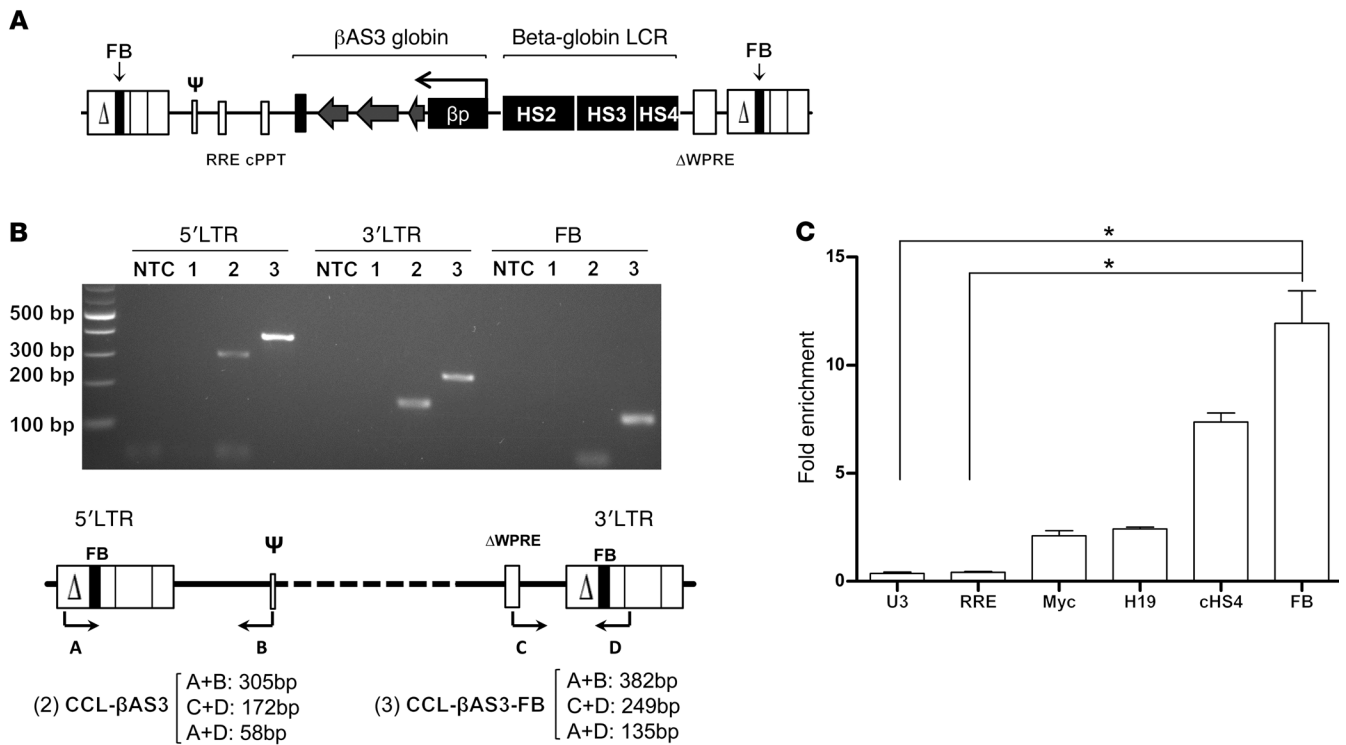
Figure 1

The CCL-βAS3-FB LV provirus carrying the *HBBAS3* cassette. (**A**) The CCL-βAS3-FB LV provirus has the *HBBAS3* expression cassette with the human β-globin gene exons (arrowheads) with the 3 substitutions to encode the HbAS3 protein, introns, the 3′ and 5′ flanking regions, and the β-globin mini-locus control region (LCR) with hypersensitive sites 2–4. The 3′ LTR contains the SIN deletion and FB insulator, both transferred during RT to the 5′ LTR of the proviral DNA. (**B**) To test FB insulator stability, PCR reactions were performed using DNA from cells collected at day 14 of in vitro culture of BM CD34+ cells: mock transduced (lane 1), transduced with the CCL-βAS3 LV (lane 2), and transduced with the CCL-βAS3-FB LV (lane 3). Primers amplified either the 5′ LTR (A to B) or the 3′ LTR (C to D) or the FB insertion sites in both LTRs (A to D) of the provirus. The expected sizes of the PCR products with these primer pairs are indicated for the CCL-βAS3 LV and the CCL-βAS3-FB LV. NTC, no template control. (**C**) CTCF-binding protein ChIP. Chromatin was isolated from K562 cells transduced with the CCL-βAS3-FB LV (FB), the CCL-βAS3-1.2 kb cHS4 LV (cHS4), or the CCL-βAS3 vector lacking the insulator (U3). qPCR amplification was done using primers to the HIV SIN LTR (U3, cHS4, and FB) and to the HIV RRE region of the vector backbone (RRE) as negative control or the cellular c-Myc and H19/ICR sites, known to bind CTCF. *$P = 0.006$. Values shown are mean ± SD.

the extent of transduction (data not shown). Based on these findings, the CCL-βAS3-FB vector was used at a standard concentration of 2×10^7 TU/ml (MOI = 40) for all subsequent studies.

The colony-forming capacities of BM CD34+ cells were similar for samples from SCD donors or healthy donor (HD) controls, whether transduced with the CCL-βAS3-FB vector or not, with approximately 10% of cells forming colonies when plated in methylcellulose, without significant differences between groups (in all the groups compared, $P > 0.1$, by 2-way ANOVA) (Figure 2A). We noted higher percentages of burst-forming unit erythroid (BFU-E) (erythroid) colonies in SCD samples (41.34% ± 19.87% in SCD-mock and 42.33% ± 17.79% in SCD-βAS3-FB) compared with HD samples (30.67% ± 17.06% in HD-mock and 28.62% ± 12.91% in HD-βAS3-FB) ($P = 0.048$, by 2-way ANOVA) (Figure 2B). Similar erythroid skewing of progenitor cells from the BM of SCD patients has been reported (41) and may reflect the increased level of erythropoiesis in SCD patients due to the underlying hemolytic anemia.

qPCR of individual CFU to detect the CCL-βAS3-FB vector sequences demonstrated the percentage of transduced colony-forming progenitor cells from SCD donor BM. Fifty-seven of 191 colonies contained the CCL-βAS3-FB vector (29.84% ± 16.68%

positive colonies in 5 independent experiments) with an average of 0.92 ± 0.57 VC/cell in the bulk population cultured in vitro in erythroid differentiation conditions. Most of the vector-positive colonies analyzed had 1 to 2 VC/cell (88%), while 11% had 3 to 6 VC/cell and 2% had 7 to 9 VC/cell (no colony had more than 9 copies) (Figure 2C).

After 2 weeks of culture under in vitro erythroid differentiation conditions, transduction of CD34+ cells from HD (*n* = 11) led to 1.28 ± 0.51 VC/cell compared with 0.93 ± 0.37 for SCD donors (*n* = 15), which was borderline significantly different ($P = 0.05$, Wilcoxon rank sum test) (Figure 2D).

In vitro erythroid differentiation of BM CD34+ cells. To assess expression of the erythroid specific *HBBAS3* cassette, an in vitro model for supporting erythroid-directed differentiation from human BM CD34+ cells was used (42). CD34+ cells from the BM of SCD donors and HD were transduced with the CCL-βAS3-FB LV and control samples were mock-transduced. Starting 24 hours post transduction (pTD), the cells were differentiated for 21 days. During erythroid culture, the cells were counted serially over 3 weeks to determine viability and cell expansion. No differences in cell growth were found between HD and SCD donors for cells that were either
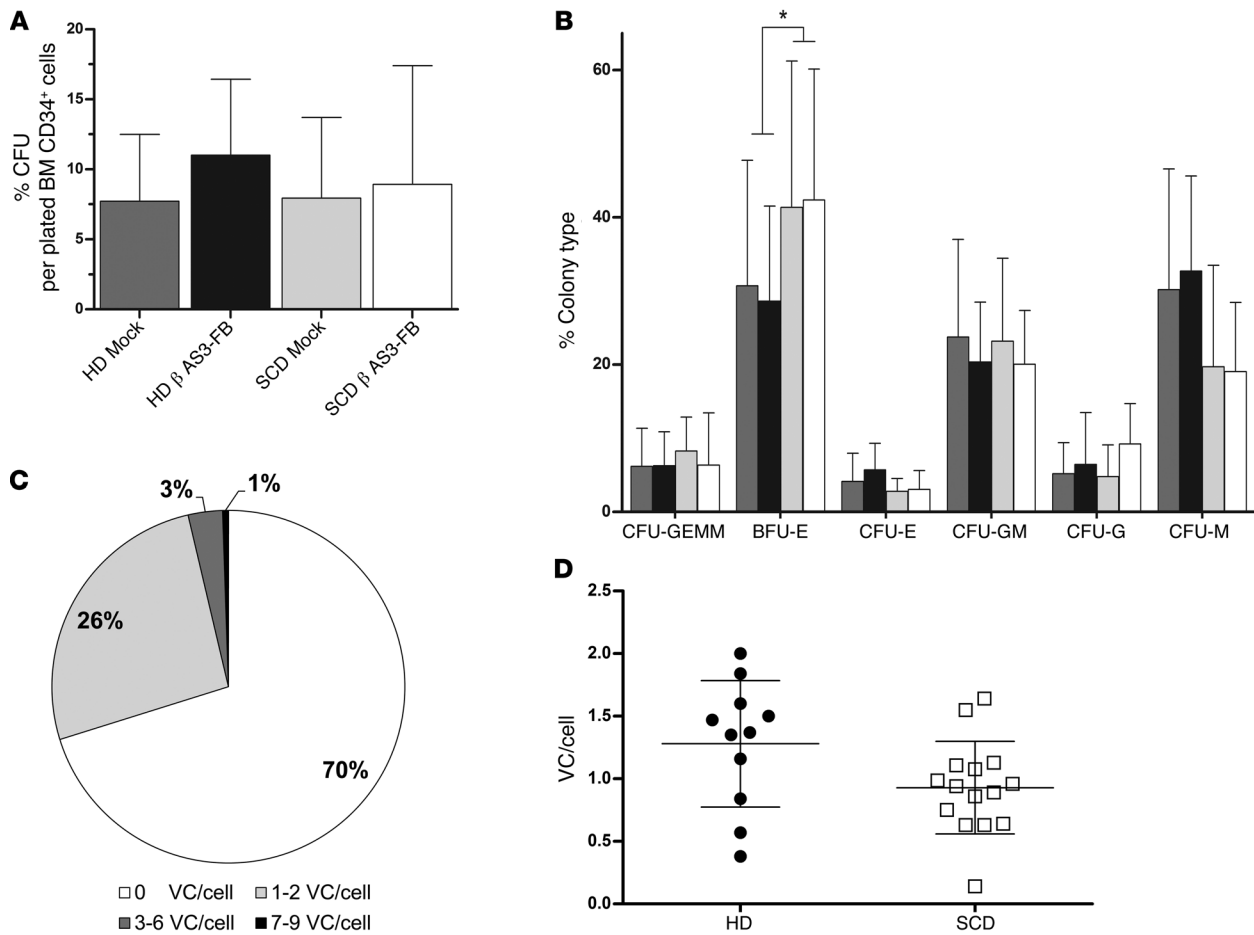
Figure 2
Assessment of transduction and hematopoietic potential of BM CD34+ cells in CFU assay and under in vitro erythroid differentiation culture. (**A**) The percentage of plated BM CD34+ cells that grew into hematopoietic colonies by in vitro CFU assay is shown. Values presented are the mean ± SD for HD-mock, *n* = 13; HD-βAS3-FB, *n* = 16; SCD-mock, *n* = 18; and SCD-βAS3-FB, *n* = 24. (**B**) Distribution of hematopoietic colony types formed by BM CD34+ cells. The percentages of the different types of hematopoietic colonies identified are represented, following the same patterns as in **A**. HD-mock, *n* = 5 independent experiments; HD-βAS3-FB, *n* = 7 independent experiments; SCD-mock, *n* = 6 independent experiments; and SCD-βAS3-FB, *n* = 8 independent experiments. Values shown are mean ± SD. **P = 0.048, by 2-way ANOVA. (**C**) In vitro single CFU grown from transduced SCD CD34+ BM were analyzed for the presence of CCL-βAS3-FB vector provirus and VC/cell by qPCR (*n* = 191 colonies, 5 independent experiments). Graph indicates percentages of the CFU that were negative for vector by qPCR (white, *n* = 134) or that had VC/cell of 1–2 (light gray, *n* = 50), 3–6 (dark gray, *n* = 6), and 7–9 (black, *n* = 1). (**D**) VC/cell for CCL-βAS3-FB-transduced BM CD34+ cells grown under in vitro erythroid differentiation culture. Each point represents an independent transduction and culture. BM CD34+ cells were from HD (black circles, *n* = 11) or SCD donors (white squares, *n* = 15). Error bars represent mean values ± SD.

transduced with the CCL-βAS3-FB LV or mock transduced (Figure 3A shows a representative experiment). Expansion of cell numbers up to 700-fold was reached by the end of the culture.

Flow cytometry was performed during erythroid differentiation culture to analyze the changes in markers of hematopoietic progenitors (CD34 and CD45) and erythroid progenitors (glycophorin A [GpA] and CD71). The percentages of CD34+ cells was analyzed after isolation, showing an average of 76.74% ± 3.01% of CD34+ cells. High variability in CD34 expression was observed after 3 days in culture between the different donors, with a sharp decline of CD34 expression between days 3 and 14 in all the samples (Figure 3B). The pan-leukocyte marker CD45 was expressed by the entire cell population at day 3 and became essentially undetectable between days 14 and 21, as expected for reticulocytes and

mature rbc (43). CD71 (transferrin receptor) was expressed during the early part of the culture period (days 3 to 14), but decreased by the end of culture period as expected (day 21). GpA expression was detected on more than 90% of the cells by day 14 and persisted until the end of the culture.

Enucleated rbc were identified at the end of the differentiation (days 18 to 21) by double staining with an antibody to the erythroid membrane glycoprotein GpA and the fluorescent dye DRAQ5, which labels DNA; enucleated rbc were defined as being GpA+DRAQ5−. The frequency of enucleated rbc among multiple cultures ranged from 65% to 85%: 67.61% ± 17.68% in SCD-mock (*n* = 7), 69.69% ± 18.11% in SCD-βAS3-FB (*n* = 7) (Figure 3B), 83.40% ± 10.07% in HD-mock (*n* = 7) and 79.04% ± 10.19% in HD-βAS3-FB (*n* = 3), without significant differences between mock-transduced
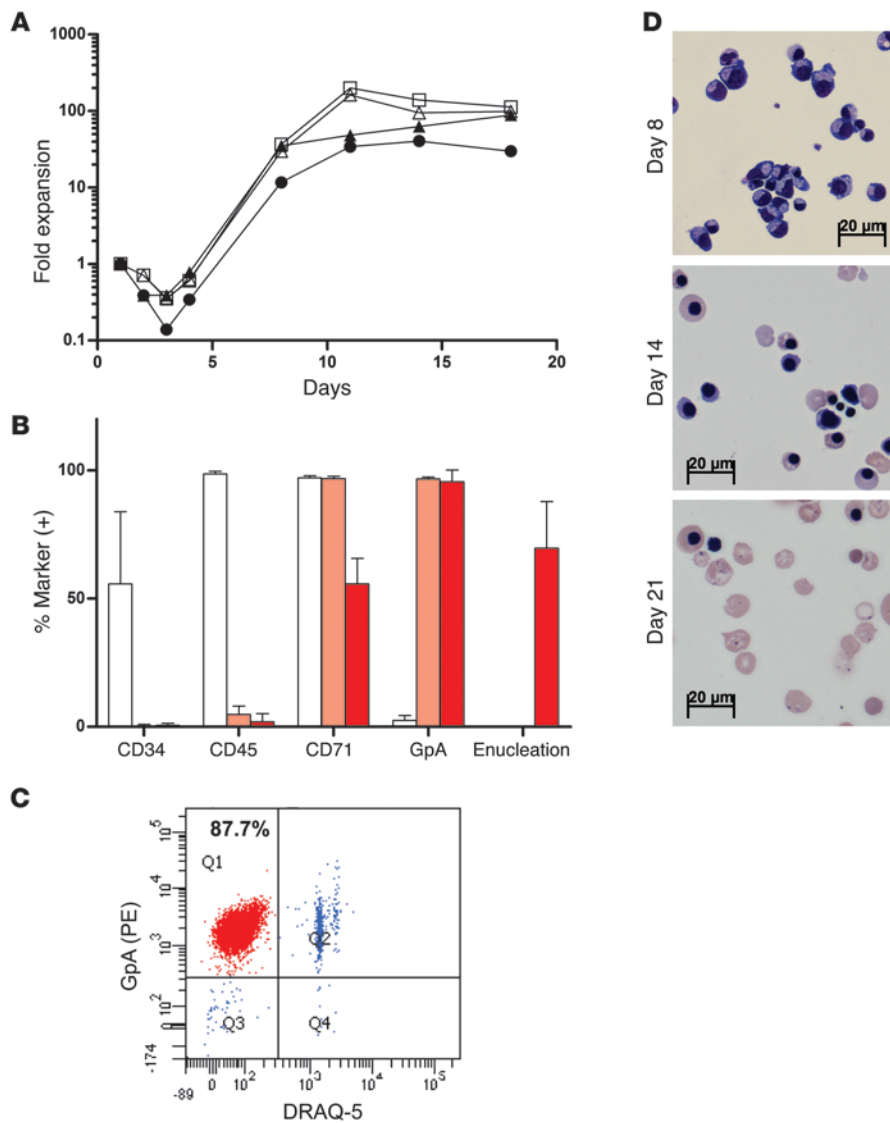
Figure 3
In vitro erythroid differentiation of BM CD34+ cells. (**A**) Fold expansion from BM CD34+ cells grown under in vitro erythroid differentiation conditions over time. The growth curves from a representative experiment are shown. HD-mock, black triangles; HD-βAS3-FB transduced, black circles; SCD-mock, white triangles; SCD-βAS3-FB transduced, white squares. (**B**) Immunophenotypic analysis of CD34+ BM SCD–transduced samples during in vitro erythroid culture. Cells were analyzed by flow cytometry for expression of CD34, CD45, CD71, and GpA. Each bar represents the percentage of expression of the indicated surface marker at day 3 (white bars), day 14 (pink bars), and day 21 (red bars). Values shown are mean ± SD of 4 independent experiments. Percentage of enucleated rbc was assessed at day 21 (mean ± SD of 7 independent experiments) by staining with the DNA dye DRAQ5. (**C**) Flow cytometry analysis of erythroid culture to quantify enucleated rbc. Analysis was made by staining cells with DRAQ5 and antibody to human erythroid marker GpA. Enucleated erythrocytes are present in the left upper quadrant as DRAQ5-negative, GpA-positive cells. (**D**) Photomicrographs of cytocentrifuge preparations from cultures stained by May-Grunwald-Giemsa showing the progression of erythroid differentiation from erythroblast to normoblast at day 8 and 14 to a mostly uniform population of enucleated reticulocytes and erythrocytes at day 21.

and LV-transduced samples (SCD mock vs. βAS3-FB, *P* = 0.80; HD mock vs. βAS3-FB, *P* = 0.69, by 2-way ANOVA). The large-cell expansion and robust erythroid differentiation with high levels of enucleation (Figure 3, C and D) supported the further analyses to characterize the activity of the *HBBAS3* transgene.

HBBAS3 mRNA expression after in vitro erythroid differentiation of BM CD34+ cells. The successful production of rbc from BM CD34+ cells plus the confirmation of efficient gene transfer allowed us to evaluate the function of the *HBBAS3* cassette. *HBBAS3* mRNA expression levels in cells collected on day 14 from in vitro erythroid differentiation cultures of SCD donor and HD BM CD34+ cells, either transduced with the CCL-βAS3-FB LV or mock transduced, were assessed by a qRT-PCR assay and compared with mRNA levels from the endogenous *HBB* and *HBBS* (*HBB* gene carrying the sickle mutation) genes. *HBBAS3* mRNA levels made up 15.73% ± 8.36% and 17.12% ± 7.25% of total β-globin–like mRNA in erythroid cells from cultures of SCD and HD BM CD34+ cells, respectively. For each CCL-βAS3-FB LV-transduced BM sample analyzed (SCD and HD), the percentage of *HBBAS3* mRNA detected was compared with the VC/cell obtained by qPCR from that sample. There was a

strong positive correlation between VC/cell and the percentage of *HBBAS3* mRNA (Pearson correlation = 0.73, P = 0.0003), indicating consistent expression (Figure 4A). When normalized to VC/cell to adjust for variable gene transfer, the average *HBBAS3* mRNA expression per VC/cell, was 26.22% ± 10.71% in SCD and 17.84% ± 11.60% in HD cells. On average, from all the samples studied (*n* = 20, 16 samples for SCD and 4 for HD) *HBBAS3* mRNA comprised 24.55% ± 11.03% per VC/cell.

Finally, we assessed the erythroid specificity of expression of the *HBBAS3* cassette by analyzing *HBBAS3* mRNA expression in CCL-βAS3-FB LV-transduced BM CD34+ cells divided into parallel cultures under myeloid and erythroid differentiation conditions. We found a higher expression of *HBBAS3* mRNA in cells produced under erythroid conditions compared with myeloid conditions, which was essentially unmeasurable (Supplemental Figure 3).

HbAS3 protein expression after in vitro erythroid-differentiation of BM CD34+ cells. We used isoelectric focusing (IEF) to examine the Hb tetramers present in erythroid cells produced in vitro from BM CD34+ cells transduced with the CCL-βAS3-FB LV. Despite the 3 amino acid differences, HbAS3 tetramers cannot be distinguished
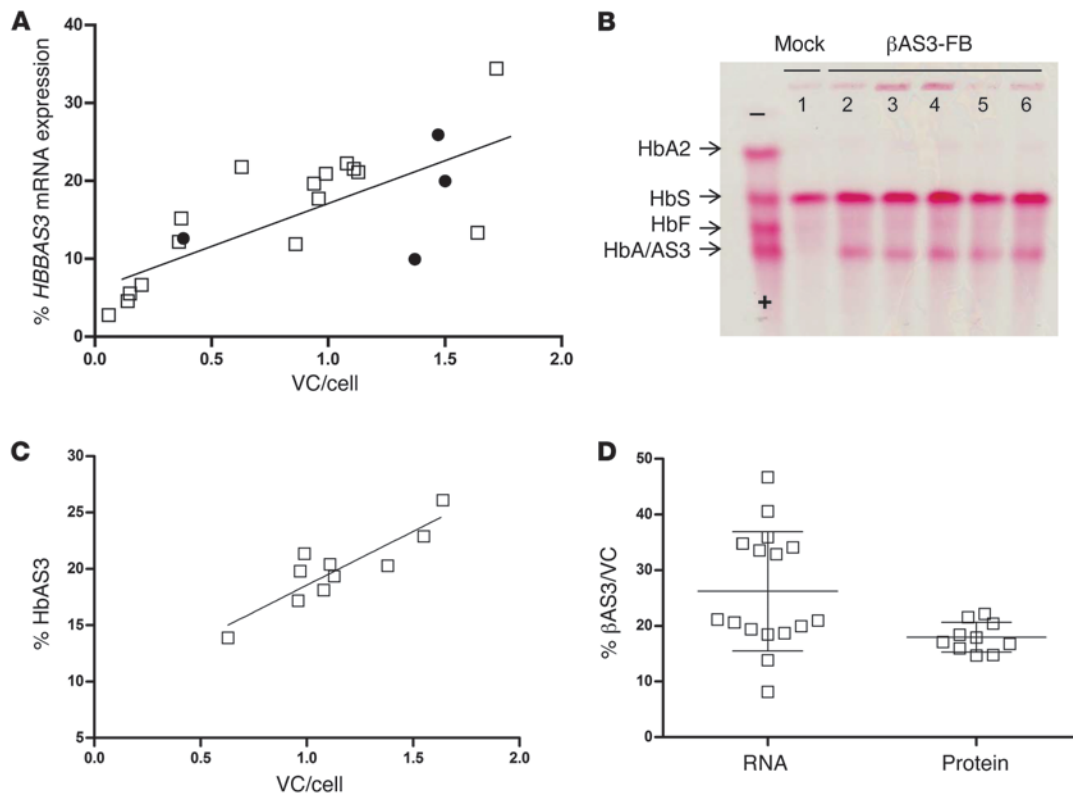
Figure 4
HBBAS3 expression after in vitro erythroid differentiation from CD34^{+} BM samples. (**A**) *HBBAS3* mRNA expression measured by qRT-PCR from cells transduced to different VC/cell. The percentage of *HBBAS3* mRNA achieved from each sample was related to its corresponding VC/cell measured by qPCR. A total of 20 independent transductions are shown. HD, black circles (*n* = 4); SCD, white squares (*n* = 16). (**B**) Representative IEF membrane used to quantify the Hb tetramers present. The left-most lane shows the pI standards of human Hb tetramers from the top down: HbA2, HbS, HbF, and HbA (and the predicted pI for HbAS3). Lanes 1–6 show the IEF of lysates from erythroid cultures initiated with SCD BM CD34^{+} cells, either mock transduced (lane 1) or transduced with the CCL-βAS3-FB LV (lanes 2–6). No HbAS3 protein was detected in the mock-transduced samples (lane 1), while HbAS3 represented of the total Hb the following: 21.78% (lane 2, 1.14 VC), 18.11% (lane 3, 1.08 VC), 19.34% (lane 4, 1.13 VC), 21.34% (lane 5, 0.99 VC), and 20.40% (lane 6, 1.11 VC). Densitometric analyses were used to determine the percentage of HbAS3 of total Hb tetramers, and qPCR was used to measure the VC/cell in the same samples. (**C**) HbAS3 protein produced from cells transduced to different VC/cell (*n* = 10). (**D**) Summary of *HBBAS3* expression per VC/cell based on measurement of *HBBAS3* mRNA (*n* = 16) and HbAS3 tetramers (protein, *n* = 10). Error bars represent mean values ± SD.

from HbA by IEF because of their identical net charge. However, HbAS3 production can be readily distinguished from HbS, as the Glu6Val substitution introduced by the canonical sickle mutation deletes a negative charge in the protein, resulting in a more positive relative net charge of HbS. Therefore, only cells from SCD donors were analyzed for HbAS3 expression by IEF.

An IEF membrane from a representative experiment is shown with 5 independent transductions of SCD BM CD34^{+} cells with the CCL-βAS3-FB LV, plus a mock-transduced sample (Figure 4B). In total, 10 SCD samples were analyzed after erythroid differentiation. There was a strong correlation between the percentage of HbAS3 present in each sample and the extent of transduction measured by the VC (Pearson correlation = 0.88, *P* = 0.001) (Figure 4C). A concomitant analysis of the some erythroid cell samples was performed by HPLC and IEF and showed similar results by both methods (Supplemental Table 1).

We then compared *HBBAS3* RNA and protein expression levels normalized per VC/cell (Figure 4D). While there was greater variability for *HBBAS3* mRNA per VC/cell values compared with protein per VC/cell, the 2 methods indicated similar values of

HBBAS3 expression (24.55% ± 11.03% *HBBAS3* mRNA per VC/cell and 17.96% ± 3.09% HbAS3 protein per VC/cell), again indicating consistent expression.

In 4 independent transductions, we compared the expression (mRNA and protein) from the *HBBAS3* cassette in the presence or absence of the FB insulator (Supplemental Figure 4). We found that the addition of the FB insulator did not alter the expression of the *HBBAS3* cassette when compared with the noninsulated LV.

SCD phenotypic correction. To assess the functional effects of *HBBAS3* expression on the sickling of rbc produced in vitro from SCD BM CD34^{+} cells, we adapted and optimized an assay used in clinical laboratories to diagnose SCD: exposure of cells to the reducing agent sodium metabisulfite to induce HbS polymerization. rbc were harvested at the end of the erythroid culture (day 21) and incubated in sealed chambers of glass slides with sodium metabisulfite. After incubation, the morphology and shapes of the individual rbc were analyzed using phase-contrast microscopy to quantify the percentages of sickled-appearing rbc (srbc) and round, discoid nonsickled normal rbc (nrbc) (Figure 5, A and B). In each experiment, 200–900 cells were analyzed for each sample.
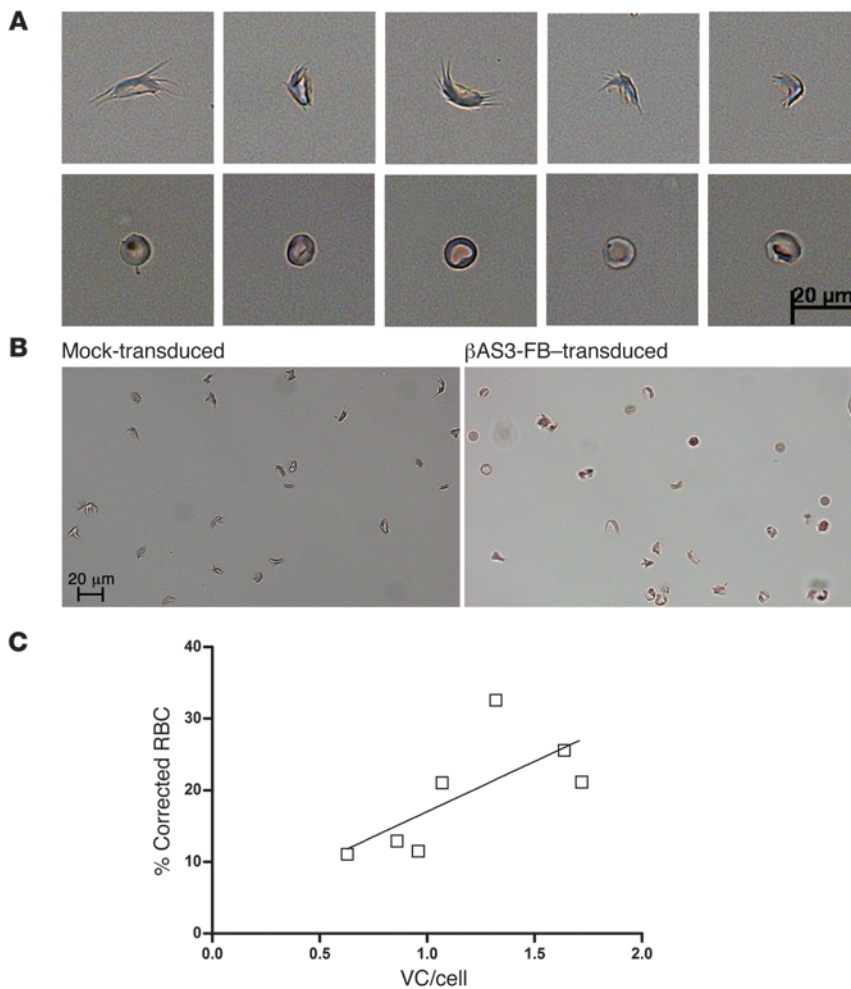
Figure 5
SCD phenotypic correction. (**A**) Phase contrast photomicrographs of deoxygenated erythroid cells. Cells from erythroid differentiation cultures of BM CD34+ cells were treated with sodium metabisulfite, and their morphology was assessed using phase contract microscopy. Five examples of srbc are displayed across the top panels, and 5 examples of nrbc are displayed across the bottom panels. (**B**) Representative field of rbc from mock-transduced SCD CD34+ cells (left panel) vs. CCL-βAS3-FB transduced SCD CD34+ cells (right panel) upon deoxygenation with sodium metabisulfite. (**C**) Correlation of the percentage of morphologically "corrected" cells to the VC/cell in each individual culture of CCL-βAS3-FB–transduced SCD BM CD34+ cells. The percentage of corrected rbc is defined as the percentage of nonsickled cells in a transduced sample minus the background value of nonsickled cells in the concordant nontransduced sample.

rbc from HD controls did not sickle in the presence of sodium metabisulfite, with more than 98% retaining their round morphology. In contrast, rbc produced in vitro from SCD BM CD34+ cells underwent sickling to a high extent in sodium metabisulfite, with averages of 88% ± 9% srbc and 12% ± 9% nrbc. In SCD samples transduced with the CCL-βAS3-FB LV, there was an increase in the percentage of rbc that did not undergo sickling, with 69% ± 16% srbc and 31% ± 16% nrbc, representing 19% ± 8% more nrbc compared with the nontransduced samples. These results demonstrated that expression by the CCL-βAS3-FB LV reduced rbc sickling during deoxygenation. The percentage of corrected sickle cells was positively correlated with the VC present (Spearman correlation = 0.77, P = 0.04) (Figure 5C and Table 1).

In vivo assessment of CCL-βAS3-FB LV transduction of BM CD34+ cells. To characterize the gene transfer and expression by the CCL-βAS3-FB LV in more primitive human hematopoietic stem and progenitor cells (HSPC), βAS3-FB–transduced BM CD34+ cells from SCD donors and HD controls were xeno-transplanted into immunodeficient NOD.Cg-*Prkdc^{scid}Il2rg^{tm1Wjl}*/SzJ (NSG) mice. Transduction conditions were the same as used for the in vitro analyses, and the cells were transplanted immediately after an overnight transduction. The transplanted cell doses ranged from 10^5 to 10^6 cells per mouse, depending on cell availability (BM source, cell dose, and number of mock- and βAS3-transduced

mice used in each transplant are provided in Table 2). Eight to twelve weeks after transplant, the mice were euthanized and the BM was harvested for FACS analysis. Human cells recovered from the NSG BM were cultured under erythroid differentiation for further analysis.

FACS analyses were performed to determine the engraftment of human cells in murine BM, defined as the percentage of human CD45+ cells of the total CD45+ population (murine CD45+ plus human CD45+). Engraftment values were variable among different transplants (up to 78%) (Figure 6A). There were not consistent differences in engraftment using BM CD34+ cells from SCD donors or HD controls (P = 0.6, by 2-way ANOVA) or between cells transduced with the βAS3-FB LV or mock-transduced (P = 0.8, by 2-way ANOVA).

The human CD45+ populations from the transplanted mice were further analyzed for expression of markers for B-lymphoid cells (CD19), myeloid progenitors (CD33), hematopoietic progenitors (CD34), and erythroid cells (CD71). There were no differences in the relative proportions of the different types of human cells between mice engrafted with mock-transduced or CCL-βAS3-FB LV-transduced BM CD34+ cells, with the majority of human cells being B lymphoid cells (Figure 6B), demonstrating that the transduction did not alter the differentiation potential of the cells.

Table 1
Enumeration of normal erythroid cells in SCD cells mock transduced and transduced with the CCL-βAS3-FB LV

Experiment no.	Donor age (yr)	% HbF	VC/cell	% nrbc SCD-Mock	% nrbc SCD-βAS3-FB	% Correction
1	8	4.70	0.63	12.8	23.9	11.1
2	8	4.05	1.64	16.7	42.2	25.6
3	12, 8, 20[A]	0	0.96	4.8	16.4	11.5
4	12	0	0.86	1.6	14.6	12.9
5	12, 18, 21, 25, 27[A]	0	1.72	3.7	24.8	21.2
6	27, 1[A]	5.40	1.07	18.7	39.8	21.1
7	12	NA	1.32	25.7	58.3	32.6

[A]Multiple SCD-BM samples were pooled for these experiments. NA, not analyzed.

BM was harvested from NSG mice, and human cells were enriched by depletion of murine CD45+ cells using immunomagnetic beads. The cells were then grown under in vitro erythroid differentiation conditions to induce terminal erythroid differentiation to allow the assessment of *HBBAS3* mRNA expression by the CCL-βAS3-FB LV vector using qRT-PCR.

The VC/cell measured in cells grown from mice engrafted with human CD45+ cells ranged from 0.05 to 0.91 (Figure 6C). Similar levels of gene marking were seen in samples from mice transplanted with BM CD34+ cells from SCD donors and HD ($P = 0.3$, by 2-sample, 2-tailed t test). Overall, the VC/cell values assessed by qPCR were highest in cells grown in vitro under erythroid differentiation conditions (1.18 ± 0.64 VC/cell), were lower in CFU (0.71 ± 0.75 VC/cell) and cells produced by in vitro myeloid differentiation cultures (0.46 ± 0.33 VC/cell), and were lowest in the human cells recovered from the NSG mice (0.34 ± 0.31 VC/cell) (Supplemental Figure 5).

Quantification of *HBBAS3* mRNA expressed by the human erythroid cells produced by in vitro erythroid differentiation of the cells isolated from the NSG mice was done using qRT-PCR. Expression of vector transcripts was correlated with VC/cells, with a mean value of 21.69% ± 8.35% of the total β-globin–like mRNA/VC (Pearson correlation = 0.89, $P = 0.0004$) (Figure 6D). Thus, expression by the CCL-βAS3-FB LV was at a level in erythroid cells differentiated from the human cells engrafted in the NSG mice similar to that in transduced BM CD34+ cells that were directly differentiated in vitro.

Genotoxicity assessment of the CCL-βAS3-FB LV. To evaluate the potential genotoxicity of the CCL-βAS3-FB LV, which contained strong erythroid enhancer elements as part of the lineage-specific β-globin expression cassette, 2 evaluations were performed: vector integration site (IS) analysis and an in vitro immortalization (IVIM) assay.

The vector IS in transduced human BM CD34+ cells were identified using nonrestrictive ligation-amplified PCR (nrLAM-PCR) and mapping of the flanking sequences to the human genome with bioinformatic analyses. Comparisons were made between the patterns of the vector integration in the transduced BM CD34+ cells after a brief in vitro expansion versus after engraftment in NSG mice to look for evidence of preferential in vivo selection of clones containing integrants near cancer-associated genes (44) or transcriptional start sites (TSS) as evidence of vector-related genotoxicity.

There were no increases in the percentages of vectors in proximity to cancer-associated genes following in vivo growth (binomial test, $P = 0.32$; P value was determined using the binomial test, taking the proportion of cancer gene–proximal IS in the in vitro condition as an estimate of the probability of observing such an IS in engrafted mice) (Figure 7A). There also was not an increased frequency of cells with vector integrations in proximity to TSS of genes (Supplemental Table 3) compared with a random data set; in contrast, a comparative vector IS data set from a clinical trial using a γ-retroviral vector (45) did show higher than random integrations near TSS (Figure 7B).

To further assess the risk of insertional transformation by the βAS3-globin LV vectors, we performed genotoxicity studies using the IVIM assay that quantifies the immortalizing events by insertional transformation of murine lineage–negative BM cells grown in limiting dilution (46). The immortalizing capacities of the LV vectors CCL-βAS3, CCL-βAS3-FB, and CCL-βAS3-cHS4 were compared with those of the γ-retroviral RSF91-GFP-wPRE as a positive control and with mock-transduced cells as a negative control. RSF91-GFP-wPRE carries the spleen focus-forming virus (SFFV) LTRs and is known to transform primary murine cells by insertional mutagenesis with a high probability in this assay.

Consistent with previous reports, the SFFV LTR–driven RSF91-GFP vector frequently generated clones (in 8 out of 14 transductions) with high replating frequencies of up to 5.26^{-02} (or 1 in 19 cells). In contrast, we found that in a total of 22 independent transductions (CCL-βAS3, $n = 4$; CCL-βAS3-FB, $n = 14$; and CCL-βAS3-cHS4, $n = 4$), the βAS3-globin LV vectors did not give rise to any clones after the replating step (Figure 7C and Supplemental Table 2). In this in vitro setting, CCL-βAS3-FB was significantly less genotoxic than the SFFV LTR–driven γ-retroviral vector RSF91-GFP ($P = 0.002$, by 2-sided Fisher's exact test) (Figure 7C).

Table 2
NSG mice transplant conditions

Transplant group	1	2	3	4	5	6
BM source	SCD	SCD	HD	HD	SCD	HD
Cell dose	9×10^4	3×10^5	10^6	5×10^5	10^6	6.3×10^5
No. mock mice	3	1	2	3	1	1
No. βAS3-FB mice	5	2	6	6	4	4
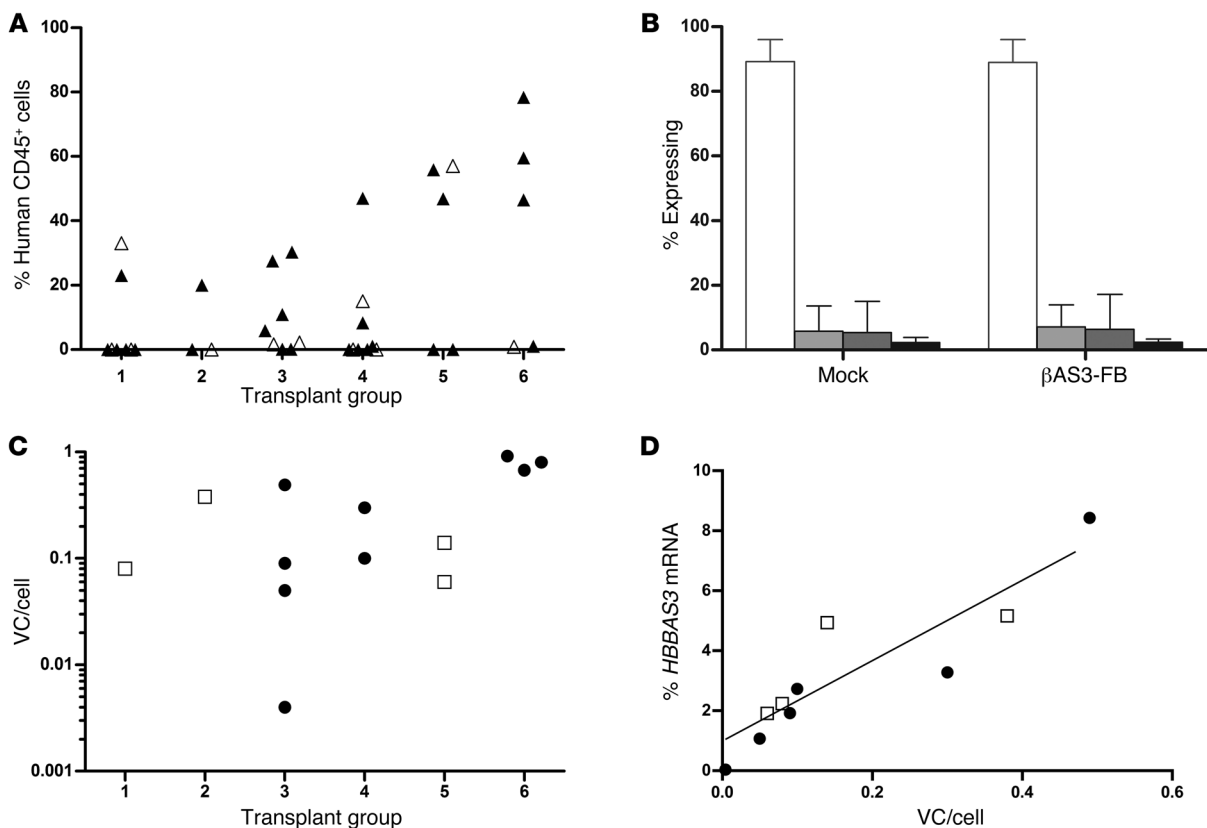
Figure 6
In vivo assessment of CCL-βAS3-FB LV transduction of BM CD34+ cells. (**A**) Engraftment of human cells in NSG mice. BM cells isolated from mice from each transplant group (nos. 1–6) were analyzed by flow cytometry to measure the percentage of human CD45+ cells among all CD45+ cells in the marrow (human and murine) as a measurement of engraftment. Mock transduced, white triangles; CCL-βAS3-FB transduced, black triangles. BM samples from HD were used in transplants 3, 4, and 6 and from SCD donors in transplants 1, 2, and 5. (**B**) Immunophenotypic analysis of human cells isolated from NSG mice transplanted with transduced BM CD34+ cells. Flow cytometry was used to enumerate the percentage of the human CD45+ cells that were positive for the markers of B-lymphoid cells (CD19, white), myeloid progenitors (CD33, light gray), hematopoietic progenitors (CD34, dark gray), and erythroid cells (CD71, black). Mean ± SD are shown of 3 independent experiments. Mock, n = 4; βAS3-FB, n = 8 mice. (**C**) VC/cell in human cells cultured from NSG mice transplanted with transduced BM CD34+ cells. Black circles represent samples from mice transplanted with HD BM, and white squares represent mice transplanted with SCD BM. All the human cells examined from mock-transduced mice were negative for VC analysis by qPCR. (**D**) HBBAS3 mRNA expression measured by qRT-PCR from cells transduced to different VC/cell. Five independent transductions are shown. HD, black circles (n = 6); SCD, white squares (n = 4).

Discussion

We performed studies using human BM CD34+ cells from SCD donors to assess the potential suitability of the CCL-βAS3-FB LV to achieve the requisite levels of transfer and expression of the anti-sickling HBBAS3 gene to inhibit sickling in rbc. BM is the likely autologous HSC source that would be used clinically for gene therapy in SCD because of the increased risks from mobilization of PBSC with G-CSF in SCD patients (10–12).

In allogeneic HSCT for SCD, stable donor HSC chimerism of 10%–30% can lead to significant hematologic and clinical improvement due to a selective survival advantage of the normal donor–derived rbc compared with the shortened survival of the HbS-containing recipient-derived rbc (47–50). In SCD patients with HPFH, levels of HbF of 8%–15% or more (24, 51) ameliorate the severity and frequency of clinical symptoms. These clinical findings define the minimum threshold for autologous transplant of gene-corrected HSC to benefit SCD because it is unknown whether rbc expressing the HBBAS3 gene will be as beneficial as rbc expressing only HBB from an HD. Hence, at least 10%–30% engrafted gene-corrected HSC producing rbc expressing at least 8%–15% HbAS3 would be needed to potentially achieve the same therapeutic effect as a similar level of allogeneic donor engraftment. Human CD34+ cells are relatively resistant to gene transfer by LV vectors compared with permissive cell lines, and this is accentuated when the vector titers are low. Thus, a key challenge is transducing a sufficient percentage of the CD34+ cells to lead to engraftment of gene-corrected HSC at the needed frequencies (e.g., 10%–30%). Stable engraftment of 10%–20% gene-modified autologous HSC has been demonstrated in clinical trials for X-ALD and β-thalassemia using LV vectors and fully cytoablative conditioning, indicating that it should be achievable in the setting of SCD as well (31, 52). In our study, the CFU assay demonstrated that 30% of the colony-forming progenitors were transduced; transduction of this percentage of engrafting HSC would be within the target range for a clinical trial, but it is not known how the frequency of lentiviral transduction measured in CFU assay correlates with the transduction frequency of HSC.
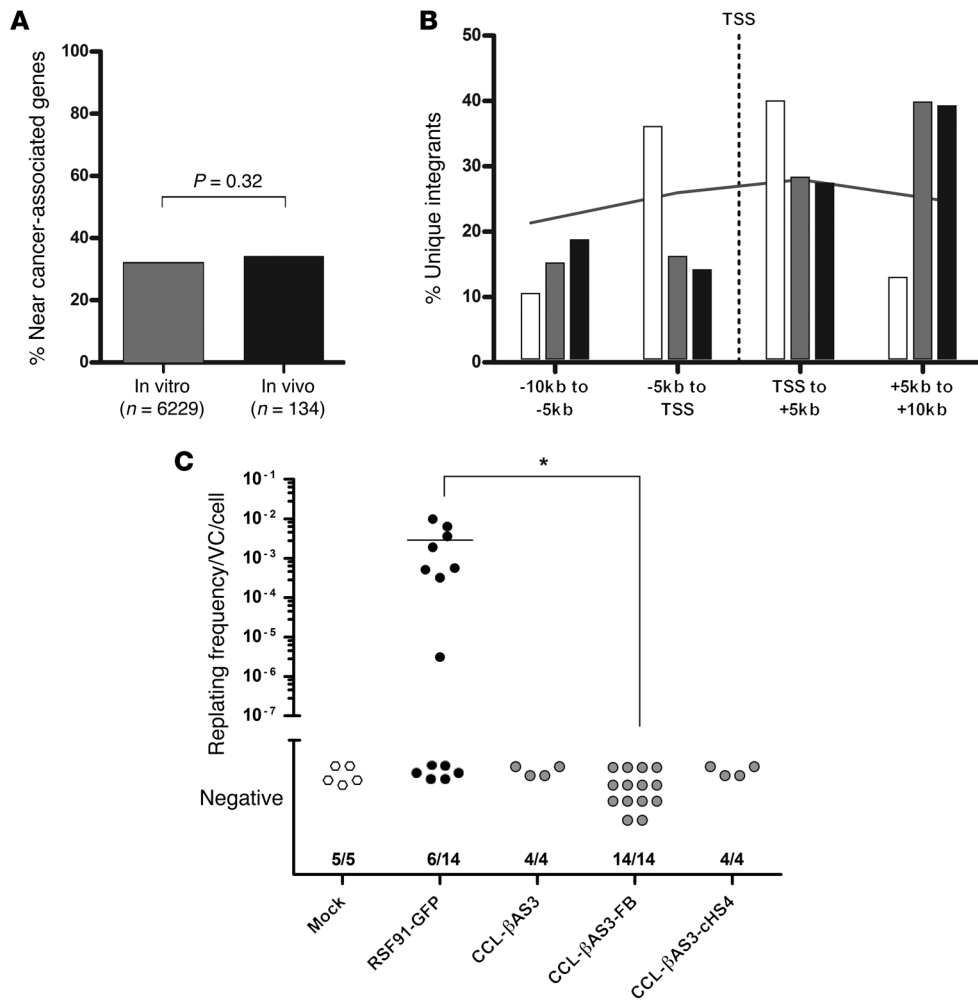
Figure 7
Assessment of genotoxicity of the CCL-βAS3-FB LV vector. (**A**) Frequency of vector IS in and near cancer-associated genes. The bars represent the frequencies of integrations in transcribed regions or within 50 kb of promoters of cancer-associated genes (in vitro, 32.1%; in vivo, 34.3%), as defined in Higgins et al. (44). (**B**) Integration frequency around TSS. The frequencies of vector IS in the four 5-kb bins in a 20-kb window centered at gene TSS are plotted. The IS are shown for the following: BM CD34+ cells analyzed after 2 weeks growth in vitro (lenti in vitro, n = 2091; gray bars) and 2–3 months in vivo engraftment in NSG mice (lenti in vivo, n = 414; black bars) along with an MLV γ-retroviral vector data set from a clinical gene therapy trial (MLV in vitro, n = 828) (45) and a random data set generated in silico and analyzed by identical methods (random, n = 12,837; black line). (**C**) IVIM assay. The replating frequencies for murine lineage-negative cells transduced with the different vectors are shown, calculated based on Poisson statistics using L-Calc software corrected for the bulk VC/cell measured by qPCR on day 8 pTD. The fractions presented across the lower portion of the figure represent the number of negative assays in which no clones were formed divided by the total number of assays performed for that vector. The horizontal bar represents the mean replating frequency of all positive assays. *P = 0.002, by 2-sided Fisher's exact test.

The anti-sickling activity of the *HBBAS3* gene was shown to be equivalent to HbF in vitro (33), so production of HbAS3 at greater than 8%–15% of total Hb levels may inhibit sickling in a clinically beneficial manner. In a murine model of SCD, the parental LV DL-βAS3 expressed HbAS3 at 20%–25% of the total Hb, with the remainder coming from the human *HBBS* transgene (19). These prior results suggest that LV-mediated transfer of the *HBBAS3* gene could be clinically efficacious in gene therapy. In our study, the expression and functional activity of the CCL-βAS3-FB LV was remarkably consistent and effective. There was a very reproducible level of expression of the *HBBAS3* gene by the vector in primary human erythroid cells produced from

transduced BM CD34+ cells, making up 15%–25% of the total β-globin–like mRNA transcripts and Hb tetramers. Expression of the HbAS3 protein consistently increased the percentage of rbc produced from CCL-βAS3-FB–transduced SCD CD34+ cells that did not sickle upon deoxygenation, indicating a functional protection similar to the effect of γ-globin expression. These results are consistent with the initial studies with the *HBBAS3* gene by Townes and colleagues, in which the parental DL-βAS3 LV corrected abnormal rbc morphology and hematologic parameters in BM-transplanted SCD mice (19).

We have achieved vector transduction levels and HbAS3 protein production within the target range; however, a high-

er percentage of HSC bearing the *HBBAS3* transgene would likely provide a larger population of rbc containing the anti-sickling HbAS3 and therefore may provide greater clinical benefit. Attempts to improve β-globin LV vectors have shown that removing β-globin regulatory elements increased titer and transduction efficiency; however, this compromised expression levels (53). Further efforts to improve the transduction efficiency of β-globin vectors without compromising their transgene expression would be an important advance in the field.

We developed and tested a derivative of the original DL-βAS3 LV (19), named CCL-βAS3-FB, replacing the HIV promoter in the 5′ LTR with the CMV enhancer/promoter to eliminate the need for expressing the HIV TAT protein during the packing process (35). This modification in the original LV backbone may improve the biosafety of the vector by eliminating the TAT gene from the packaging step. It also led to at least a 10-fold increase of the vector titers when compared with the original. However, despite this improvement, the large amount of regulatory elements needed for high-level expression of the β-globin gene makes this type of LV complex and lowers the achievable titers when compared with vectors with simpler gene cassettes.

In some gene therapy settings in which strong enhancers and other regulatory elements are needed for sufficient expression of a transferred gene (e.g., chronic granulomatous disease, β-thalassemia), the genotoxic potential of these elements may be diminished when insulator elements are added (54). Insulators are DNA sequences that act as boundary elements to inhibit interactions between adjacent chromatin domains, which can manifest as either enhancer-blocking activity, heterochromatin barrier activity, or both. The enhancer-blocking activity of insulators would reduce *trans*-activation of transcription from promoters of adjacent cellular genes. The barrier activity of insulators would decrease transgene silencing caused by spreading of surrounding heterochromatin into the vector provirus (55).

The major DNA-binding protein associated with enhancer-blocking activity of insulators in vertebrates is the CTCF (CCCTC-binding factor) protein (38), a highly conserved and ubiquitous zinc finger protein (56–58). The FB insulator used in the CCL-βAS3-FB LV was previously shown to have enhancer-blocking activity similar to the full 1.2-kb cHS4 insulator in a reporter plasmid transfection assay and exceeding that of the 250-bp core cHS4 insulator fragment (36).

In the CCL-βAS3-FB LV, the relatively small FB insulator (77 bp) did not lower the titers of the parental CCL-βAS3 LV when inserted into the U3 region of the 3′ LTR. It was transmitted faithfully to the 5′ LTR during reverse transcription, with no detectable deletion or losses in the vector provirus by Southern blot analysis or by PCR analysis of the FB insulator region from pools of transduced human CD34+ cells and from clonal CFUs grown in vitro. We could not assess the functional ability of the FB insulator to decrease risks for genotoxicity in the IVIM assay because neither the parental vector lacking the FB insulator nor the CCL-βAS3-FB LV caused any clonal outgrowth. However, we did observe evidence of in vitro activity of the FB insulator based on the greatly enriched binding of CTCF protein to LTR regions of the CCL-βAS3-FB, as assessed by ChIP analysis from K562 cells.

In light of the recent report of aberrant splicing into the 250-bp cHS4 insulator element in an LV vector used for transduction of BM CD34+ cells in a trial for β-thalassemia (31), we performed an in silico splice site analysis of the FB insulator sequences. Whereas the NetGene2 server (59) identified the cryptic splicing site seen in the cHS4 insulator by Cavazzana-Calvo et al. (31), it did not predict splicing signals in an FB-containing SIN LTR. These studies indicate that the FB insulator does not lower vector titers, is transmitted intact, binds the major cellular factor responsible for producing enhancer-blocking activity, and is not predicted to serve as a cryptic splice site; however, it is unknown whether the presence of the FB insulator in the vector will increase safety in clinical applications.

Safety assessments using the IVIM assay with CCL-βAS3-FB–transduced murine BM cells and vector IS analyses of human BM CD34+ cells transplanted in vivo to NSG mice did not reveal any evidence of genotoxicity, although the sensitivity of these surrogate assays may be relatively low. The observed pattern of vector IS for the LV was consistent with those described previously for HIV-1-based LV vectors, with preferential integration into genes and no preference for integrations near TSS (60). This contrasted with a recently published γ-retroviral IS data set (45).

In all, these studies provide preclinical data for sufficiently effective transduction of human BM CD34+ progenitor from SCD patients to support translation to a clinical trial of gene therapy for SCD using the CCL-βAS3-FB LV. Subsequent steps will involve defining components of a clinical trial, such as treatment plan, subject eligibility, end points, and other study parameters to support regulatory submissions, performing cell processing scale-up, further assessing toxicology, and developing the clinical reagents. Outcomes from autologous transplants of gene-modified HSC will need to be compared with those from allogeneic transplant approaches, which continue to advance, to define the clinical utility of gene therapy for SCD.

Methods

BM CD34+ cell LV transduction. For transduction, BM CD34+ cell samples from SCD and HD were thawed and plated at 1×10^6 cells/ml in tissue culture plates precoated with RetroNectin (20 μg/ml, Takara Shuzo Co.). Prestimulation was performed for 18–24 hours in X-Vivo 15 medium (Lonza) containing 1× glutamine, penicillin, and streptomycin (Gemini Bio-Products). Cytokines were added at the following concentrations: 50 ng/ml human SCF (hSCF) (StemGent), 50 ng/ml human hFlt3 ligand (hFlt3-l) (PeproTech), 50 ng/ml human thrombopoietin (hTPO), and 20 ng/ml human IL-3 (hIL-3) (both from R&D Systems). Cells were transduced with concentrated viral supernatants of the CCL-βAS3-FB LV at a final concentration of 2×10^7 TU/ml (MOI = 40, based on titers on HT29 cells) for all experiments done. Twenty-four hours after transduction, the cells were plated in methylcellulose for CFU assay and were also plated in in vitro erythroid differentiation culture and used for xeno-transplant into NSG mice.

In vitro erythroid differentiation culture. The in vitro erythroid differentiation technique used is based on a 3-phase protocol adapted from Giarratana et al. (42). After 2 days of culture, for prestimulation and transduction, cells were transferred into erythroid culture. The basic erythroid medium was Iscove's Modified Dulbecco's Medium (IMDM; Life Technologies) (1× glutamine, penicillin, and streptomycin) supplemented with 10% BSA, 40 μg/ml inositol, 10 μg/ml folic acid, 1.6 μM monothioglycerol, 120 μg/ml transferrin, and 10 μg/ml insulin (all from Sigma-Aldrich). During the first phase (6 days), the cells were cultured in the presence of 10^{-6} M hydrocortisone (Sigma-Aldrich), 100 ng/ml hSCF, 5 ng/ml hIL-3, and 3 IU/ml erythropoietin (Epo) (Janssen Pharmaceuticals). In the second phase (3 days), the cells were transferred onto a stromal cell layer (MS-5, murine stromal cell line (61) (provided by Gay Crooks, UCLA) with the addition of only Epo (3 IU/ml) to basic erythroid medium. At day 11, all the cytokines were removed from the medium and the cells were cocultured on the MS-5 stromal layer until days 18 to 21.

qPCR for determination of VC/cell. On day 14 of the erythroid differentiation, 10^5 cells from the erythroid cultures were harvested for genomic DNA isolation using the PureLink Genomic DNA Mini Kit (Invitrogen). The average VC/cell was determined by multiplex qPCR of the HIV-1 packaging signal sequence (Psi) in the LV provirus and normalized to the cellular autosomal gene syndecan 4 (*SDC4*) to calculate the average VC/cell. This multiplex qPCR method was previously described (62).

HBBAS3 mRNA quantification by qRT-PCR. To determine *HBBAS3* mRNA expression, 1 to 2×10^5 cells were harvested on day 14 of erythroid differentiation. RNA was extracted using the RNeasy Plus Mini Kit (QIAGEN) according to the manufacturer's instructions. The genomic DNA elimination columns contained in the kit were used to eliminate possible DNA contamination during the extraction. First-strand cDNA was synthesized using random primers, M-MLV reverse transcriptase, and RNAseOUT Recombinant Ribonuclease Inhibitor (all from Invitrogen) according to the manufacturer's protocol. SYBR Green qPCR amplification of cDNAs was performed using Platinum Taq DNA Polymerase (Platinum SYBR Green qPCR SuperMix; Invitrogen) on a ViiA7 Real-Time PCR System (Applied Biosystems).

To specifically detect mRNA transcripts originating from the vector CCL-βAS3-FB (*HBBAS3* mRNA) in differentiated rbc and compare them with the levels of endogenous β-globin–like mRNA (*HBB* in HD samples and *HBBS* in SCD samples, respectively), 2 sets of allele-specific primers were designed (HBB^A/HBB^S and HBB^AS3; Supplemental Table 4). The percentage of *HBBAS3* transcripts (%*HBBAS3*) among all β-globin–like transcripts was determined from the relative expression of *HBBAS3* vs. *HBB* and *HBBS* transcripts, respectively, comparing absolute numbers of transcripts per µl cDNA measured using an absolute plasmid standard curve ranging from 10^8 to 10^1 molecules/µl DNA. Both primer sets were used in a 2-step PCR protocol with the denaturation step at 95°C for 15 seconds and the annealing/extension step at 72°C for 1 minute for a total of 40 cycles. All reactions were performed in duplicate, and dissociation curve analysis was carried out for each reaction to rule out nonspecific amplification.

HbAS3 tetramer quantification by IEF. Hb IEF was performed using the Hemoglobin Electrophoresis Procedure (Helena Laboratories) according to the manufacturer's instructions. Briefly, a minimum of 3×10^6 cells were harvested on day 21 of erythroid differentiation. The cells were lysed with Hemolysate Reagent (Helena Laboratories) as per instructions and incubated overnight at 4°C. If necessary, lysates were concentrated the next day using Micron Centrifugal Filters (Ultracel YM-30; Millipore); 5 µl of the samples were loaded onto a Titan III cellulose acetate plate (Helena Laboratories) and electrophoresed for 25 minutes at 350 volts. The plate was stained by Ponceau S (Sigma-Aldrich) for visualization of the Hb tetramers, cleared using Clear Aid solution (Helena Laboratories), and dried. The Hb bands were identified by comparison with Helena Hemo Controls and quantified by densitometry using ImageQuant TL software (GE Healthcare).

SCD phenotypic correction assay. At day 21 of the erythroid differentiation, 2.5×10^5 cells per condition were harvested for SCD phenotypic correction assay. The samples were spun down (500 *g* for 5 minutes), and the resulting pellets were harvested in 10 µl of the supernatant; 10 µl of 20 µg/ml Sodium Metabisulfite (Sigma-Aldrich) was added to each sample. This mix was loaded onto a glass microscope slide, covered, and sealed at the edges. The samples were incubated at 5% CO_2, 37°C for 25–40 minutes. Images of the cells were then captured by inverse microscopy with a Nikon DS-Fi1 camera, from consecutive fields at ×10 magnification. Computer vision was utilized to isolate cells within each field and then individually present them to the user for visual analysis of normal or sickle morphology in a randomized and unbiased fashion across treatment groups.

Transplantation of transduced human BM CD34+ cells in immunodeficient mice. BM CD34+ cells from HD or SCD donors transduced with the CCL-βAS3-FB vector or mock transduced (10^5–10^6 cells) were transplanted by tail-vein injection into 9- to 12-week-old, NSG mice (The Jackson Laboratory) after 250 cGy total body irradiation. After 8–12 weeks, mice were euthanized and BM was analyzed for engraftment of human cells by flow cytometry using APC-conjugated anti-human CD45 vs. FITC-conjugated anti-murine CD45. After antibody incubation, rbc were lysed using BD FACS-Lysing Solution (BD Biosciences). The percentage of engrafted human cells was defined as follows: %huCD45+/(%huCD45+ + %muCD45+). Analysis of the different hematopoietic cell types present was performed by staining for peridinin-chlorophyll–conjugated (PerCP) anti-human CD34, V450-conjugated anti-human CD45, FITC-conjugated anti-human CD19, PE-conjugated anti-human CD33, and APC-conjugated anti-human CD71 (all antibodies from BD Biosciences). BM from engrafted mice was depleted of murine CD45+ cells using immunomagnetic separation (CD45 MicroBeads — mouse; Miltenyi Biotech, Bergisch Gladbach). The mCD45-negative fraction was cultured for in vitro erythroid differentiation as described above to produce cells for analysis of the VC/cell and *HBBAS3* mRNA expression. For each sample, qPCR was performed using primers to amplify the packaging (Psi) region of the provirus and normalized for DNA copy using primers to the autosomal human gene *SDC4* (62) to adjust for the potential presence of murine cells in the cultures.

Vector IS analysis. Depending on availability, 1–100 ng of genomic DNA isolated from cells were used to perform nonrestrictive linear amplification–mediated (nr-LAM) PCR to identify vector IS (63). Briefly, 100 cycles of linear amplification were performed with primer HIV3 linear (biotin-AGTAGTGTGTGCCCGTCTGT). Linear reactions were purified using 1.5 volumes of AMPure XP beads (Beckman Genomics) and captured onto M-280 Streptavidin Dynabeads (Invitrogen Dynal). Captured ssDNA was ligated to read 2 linker (phos-AGATCGGAAGAGCACAC-GTCTGAACTCCAGTCAC-3C spacer) using CircLigase II (Epicentre) in a 10-µl reaction at 65° for 2 hours. PCR was performed on these beads using primer HIV3 right (AATGATACGGCGACCACCGAGATCTA-CACTGATCCCTCAGACCCTTTTAGTC) and an appropriate indexed reverse primer (CAAGCAGAAGACGGCATACGAGAT-index-GTGACTG-GAGTTCAGACGTGT). PCR products were mixed and quantified by probe-based qPCR, and appropriate amounts were used to load Illumina v3 flow cells. Paired-end 50-bp sequencing was performed on an Illumina HiSeq 2000 instrument using a custom read 1 primer (CCCT-CAGACCCTTTTAGTCAGTGTGGAAAATCTCTAGCA). Reads were aligned to the hg19 build of the human genome with Bowtie (64), and alignments were condensed and annotated using custom Perl and Python scripts to locate vector integrations relative to RefSeq gene annotations obtained from the UCSC database. The frequencies of IS in transcribed regions of or within 50 kb of promoters of cancer-associated genes (as defined in Higgins et al., ref. 44) were determined.

See Supplemental Methods for details of LV vector construction, production and titration, PCR for FB insulator integrity, Southern blot, ChIP, BM CD34+ cell isolation, CFU progenitor assay, myeloid culture, flow cytometry during erythroid culture, IVIM assay, and *HBBAS3* mRNA expression in erythoid and myeloid conditions.

Statistics. Descriptive statistics of continuous outcome variables such as the mean and SD by experimental conditions are presented in figures. For continuous outcomes such as titer, VC/cell, percentage of enucleation, percentage of colonies grown, etc., 1-way or 2-way ANOVA (65) was used to assess overall group difference, depending on the experimental designs. Further, we performed 2-group comparison by 2-sample *t* test (within the framework of ANOVA if more than 2 groups) or Wilcoxon rank sum test if normality assumption was not met. Pearson correlation

(66) was used to measure the correlation between VC/cell and percentage of *HBBAS3* mRNA and correlation of VC/cell and percentage of HbAS3; Spearman correlation (67) was used to evaluate the correlation of the VC/cell with the percentage of corrected sickle cell. For binary outcome, such as the replating condition in the IVIM assay (positive vs. negative), Fisher's exact test (68) was used to compare CCL-βAS3-FB vector with RSF91-GFP vector. To compare the proportions of IS near cancer-related genes in cells grown in vitro with cells engrafted in mice, a binomial test was performed using the proportion of cancer gene–proximal IS in the in vitro condition as an estimate of the probability of observing such an IS in engrafted mice. For all statistical investigations, tests for significance were 2 tailed. $P < 0.05$ was considered to be statistically significant. All statistical analyses were carried out using SAS version 9.3 (69), GraphPad Prism version 5.0d (GraphPad Software Inc.), and MATLAB version 7.12.0.635 (MathWorks Inc.).

Study approval. All human samples have been used following UCLA IRB protocol #10-001399. Written informed consent was obtained from the subjects used in these studies. All work with mice was done under protocols approved by the UCLA Animal Care Committee.

Address correspondence to: Donald B. Kohn, Departments of Microbiology, Immunology and Molecular Genetics and Pediatrics, University of California, Los Angeles, 3163 Terasaki Life Science Building, 610 Charles E. Young Drive South, Los Angeles, California 90095, USA. Phone: 310.794.1964; Fax: 310.206.0356; E-mail: dkohn@mednet.ucla.edu.

1. Hoffman R, et al. *Hematology: Basic Principles and Practice*. 5th ed. London, United Kingdom: Churchill Livingstone; 2009.
2. Voskaridou E, et al. The effect of prolonged administration of hydroxyurea on morbidity and mortality in adult patients with sickle cell syndromes: results of a 17-year, single-center trial (LaSHS). *Blood*. 2010;115(12):2354–2363.
3. Eaton WA, Hofrichter J. Hemoglobin S gelation and sickle cell disease. *Blood*. 1987;70(5):1245–1266.
4. Stamatoyannopoulos G, Majerus PW, Perlmutter RM, Varmus H, eds. *Molecular Basis of Blood Diseases*. 3rd ed. Philadelphia, Pennsylvania, USA: WB Saunders; 2001.
5. Bolaños-Meade J, Brodsky RA. Blood and marrow transplantation for sickle cell disease: overcoming barriers to success. *Curr Opin Oncol*. 2009;21(2):158–161.
6. Rees DC, Williams TN, Gladwin MT. Sickle-cell disease. *Lancet*. 2010;376(9757):2018–2031.
7. Shenoy S. Hematopoietic stem cell transplantation for sickle cell disease: current practice and emerging trends. *Hematology Am Soc Hematol Educ Program*. 2011;2011:273–279.
8. Kamani NR, et al. Unrelated donor cord blood transplantation for children with severe sickle cell disease: results of one cohort from the phase II study from the Blood and Marrow Transplant Clinical Trials Network (BMT CTN). *Biol Blood Marrow Transplant*. 2012;18(8):1265–1272.
9. Locatelli F, Pagliara D. Allogeneic hematopoietic stem cell transplantation in children with sickle disease. *Pediatr Blood Cancer*. 2012;59(2):372–376.
10. Abboud M, Laver J, Blau CA. Granulocytosis causing sickle-cell crisis. *Lancet*. 1998;351(9107):959.
11. Adler BK, et al. Fatal sickle cell crisis after granulocyte colony-stimulating factor administration. *Blood*. 2001;97(10):3313–3314.
12. Fitzhugh CD, Hsieh MM, Bolan CD, Saenz C, Tisdale JF. Granulocyte colony-stimulating factor (G-CSF) administration in individuals with sickle cell disease: time for a moratorium? *Cytotherapy*. 2009;11(4):464–471.
13. Neumayr L, et al. Surgery in patients with hemoglobin SC disease. Preoperative Transfusion in Sickle Cell Disease Study Group. *Am J Hematol*. 1998;57(2):101–108.
14. Lisowski L, Sadelain M. Current status of globin gene therapy for the treatment of β-thalassaemia. *Br J Haematol*. 2008;141(3):335–345.
15. Gelinas RE, Bender MA, Miller AD, Novak U. Long-term expression of the human β-globin gene after retroviral transfer into pluripotent hematopoietic stem cells of the mouse. *Adv Exp Med Biol*. 1989;271:135–148.
16. Gelinas RE, Bender MA, Miller AD, Novak U. Regulated expression of the human β-globin gene after retroviral transfer into murine and human hematopoietic cells. *Prog Clin Biol Res*. 1989;316B:235–249.
17. May C, et al. Therapeutic haemoglobin synthesis in β-thalassaemic mice expressing lentivirus-encoded human β-globin. *Nature*. 2000;406(6791):82–86.
18. Pawliuk R, et al. Correction of sickle cell disease in transgenic mouse models by gene therapy. *Science*. 2001;294(5550):2368–2371.
19. Levasseur DN, Ryan TM, Pawlik KM, Townes TM. Correction of a mouse model of sickle cell disease: lentiviral/antisickling β-globin gene transduction of unmobilized, purified hematopoietic stem cells. *Blood*. 2003;102(13):4312–4319.
20. Hanawa H, Hargrove PW, Kepes S, Srivastava DK, Nienhuis AW, Persons DA. Extended β-globin locus control region elements promote consistent therapeutic expression of a γ-globin lentiviral vector in murine β-thalassemia. *Blood*. 2004;104(8):2281–2290.
21. Puthenveetil G, et al. Successful correction of the human β-thalassemia major phenotype using a lentiviral vector. *Blood*. 2004;104(12):3445–3453.
22. Miccio A, et al. In vivo selection of genetically modified erythroblastic progenitors leads to long-term correction of β-thalassemia. *Proc Natl Acad Sci U S A*. 2008;105(30):10547–10552.
23. Pestina TI, Hargrove PW, Jay D, Gray JT, Boyd KM, Persons DA. Correction of murine sickle cell disease using γ-globin lentiviral vectors to mediate high-level expression of fetal hemoglobin. *Mol Ther*. 2008;17(2):245–252.
24. Platt OS, et al. Mortality in sickle cell disease. Life expectancy and risk factors for early death. *N Engl J Med*. 1994;330(23):1639–1644.
25. Chakalova L, et al. The Corfu deltaβ-thalassemia deletion disrupts γ-globin gene silencing and reveals post-transcriptional regulation of HbF expression. *Blood*. 2005;105(5):2154–2160.
26. Russell JE. A post-transcriptional process contributes to efficient γ-globin gene silencing in definitive erythroid cells. *Eur J Haematol*. 2007;79(6):516–525.
27. Persons DA, Hargrove PW, Allay ER, Hanawa H, Nienhuis AW. The degree of phenotypic correction of murine β-thalassemia intermedia following lentiviral-mediated transfer of a human γ-globin gene is influenced by chromosomal position effects and vector copy number. *Blood*. 2002;101(6):2175–2183.
28. Perumbeti A, et al. A novel human γ-globin gene vector for genetic correction of sickle cell anemia in a humanized sickle mouse model: critical determinants for successful correction. *Blood*. 2009;114(6):1174–1185.
29. Breda L, et al. Therapeutic hemoglobin levels after gene transfer in β-thalassemia mice and in hematopoietic cells of β-thalassemia and sickle cells disease patients. *PLoS One*. 2012;7(3):e32345.
30. Nagel RL, et al. Structural bases of the inhibitory effects of hemoglobin F and hemoglobin A2 on the polymerization of hemoglobin S. *Proc Natl Acad Sci USA*. 1979;76(2):670–672.
31. Cavazzana-Calvo M, et al. Transfusion independence and HMGA2 activation after gene therapy of human β-thalassaemia. *Nature*. 2010;467(7313):318–322.
32. McCune SL, Reilly MP, Chomo MJ, Asakura T, Townes TM. Recombinant human hemoglobins designed for gene therapy of sickle cell disease. *Proc Natl Acad Sci USA*. 1994;91(21):9852–9856.
33. Levasseur DN, Ryan TM, Reilly MP, McCune SL, Asakura T, Townes TM. A recombinant human hemoglobin with anti-sickling properties greater than fetal hemoglobin. *J Biol Chem*. 2004;279(26):27518–27524.
34. Giarratana MC, et al. Ex vivo generation of fully mature human RBCs from hematopoietic stem cells. *Nat Biotechnol*. 2004;23(1):69–74.
35. Dull T, et al. A third-generation lentivirus vector with a conditional packaging system. *J Virol*. 1998;72(11):8463–8471.
36. Ramezani A, Hawley TS, Hawley RG. Combinatorial incorporation of enhancer-blocking components of the chicken β-globin 5′HS4 and human T-cell

receiver alpha/delta BEAD-1 insulators in self-inactivating retroviral vectors reduces their genotoxic potential. *Stem Cells*. 2008;26(12):3257–3266.

37. Sastry L, Johnson T, Hobson MJ, Smucker B, Cornetta K. Titering lentiviral vectors: comparison of DNA, RNA and marker expression methods. *Gene Ther*. 2002;9(17):1155–1162.

38. Bell AC, West AG, Felsenfeld G. The protein CTCF is required for the enhancer blocking activity of vertebrate insulators. *Cell*. 1999;98(3):387–396.

39. Witcher M, Emerson BM. Epigenetic silencing of the p16(INK4a) tumor suppressor is associated with loss of CTCF binding and a chromatin boundary. *Mol Cell*. 2009;34(3):271–284.

40. Bell AC, Felsenfeld G. Methylation of a CTCF-dependent boundary controls imprinted expression of the Igf2 gene. *Nature*. 2000;405(6785):482–485.

41. Croizat H, Nagel RL. Circulating BFU-E in sickle cell anemia: relationship to percent fetal hemoglobin and BPA-like activity. *Exp Hematol*. 1988;16(11):946–949.

42. Douay L, Giarratana MC. Ex vivo generation of human red blood cells: a new advance in stem cell engineering. *Methods Mol Biol*. 2009;482:127–140.

43. Migliaccio G, et al. In vitro mass production of human erythroid cells from the blood of normal donors and of thalassemic patients. *Blood Cells Mol Dis*. 2002;28(2):169–180.

44. Higgins ME, Claremont M, Major JE, Sander C, Lash AE. CancerGenes: a gene selection resource for cancer genome projects. *Nucleic Acids Res*. 2007;35(Database issue):D721–D726.

45. Candotti F, et al. Gene therapy for adenosine deaminase-deficient severe combined immunodeficiency: clinical comparison of retroviral vectors and treatment plans. *Blood*. 2012;1(18):3635–3646.

46. Modlich U, et al. Cell-culture assays reveal the importance of retroviral vector design for insertional genotoxicity. *Blood*. 2006;108(8):2545–2553.

47. Walters MC, et al. Stable mixed hematopoietic chimerism after bone marrow transplantation for sickle cell anemia. *Biol Blood Marrow Transplant*. 2001;7(12):665–673.

48. Andreani M, et al. Quantitatively different red cell/nucleated cell chimerism in patients with long-term, persistent hematopoietic mixed chimerism after bone marrow transplantation for thalassemia major or sickle cell disease. *Haematologica*. 2010;96(1):128–133.

49. Wu CJ, et al. Mixed haematopoietic chimerism for sickle cell disease prevents intravascular haemolysis. *Br J Haematol*. 2007;139(3):504–507.

50. Krishnamurti L, et al. Stable long-term donor engraftment following reduced-intensity hematopoietic cell transplantation for sickle cell disease. *Biol Blood Marrow Transplant*. 2008;14(11):1270–1278.

51. Charache S, Dover GJ, Moyer MA, Moore JW. Hydroxyurea-induced augmentation of fetal hemoglobin production in patients with sickle cell anemia. *Blood*. 1987;69(1):109–116.

52. Cartier N, et al. Hematopoietic stem cell therapy with a lentiviral vector in X-linked adrenoleukodystrophy. *Science*. 2009;326(5954):818–823.

53. Lisowski L, Sadelain M. Locus control region elements HS1 and HS4 enhance the therapeutic efficacy of globin gene transfer in β-thalassemic mice. *Blood*. 2007;110(13):4175–4178.

54. Emery DW, Yannaki E, Tubb J, Stamatoyannopoulos G. A chromatin insulator protects retrovirus vectors from chromosomal position effects. *Proc Natl Acad Sci USA*. 2000;97(16):9150–9155.

55. Raab JR, Kamakaka RT. Insulators and promoters: closer than we think. *Nat Rev Genet*. 2010;11(6):439–446.

56. Lobanenkov VV, et al. A novel sequence-specific DNA binding protein which interacts with three regularly spaced direct repeats of the CCCTC-motif in the 5′-flanking sequence of the chicken c-myc gene. *Oncogene*. 1990;5(12):1743–1753.

57. Filippova GN, et al. An exceptionally conserved transcriptional repressor, CTCF, employs different combinations of zinc fingers to bind diverged promoter sequences of avian and mammalian c-myc oncogenes. *Mol Cell Biol*. 1996;16(6):2802–2813.

58. Vostrov AA, Quitschke WW. The zinc finger protein CTCF binds to the APBβ domain of the amyloid β-protein precursor promoter. Evidence for a role in transcriptional activation. *J Biol Chem*. 1997;272(52):33353–33359.

59. Brunak S, Engelbrecht J, Knudsen S. Prediction of human mRNA donor and acceptor sites from the DNA sequence. *J Mol Biol*. 1991;220(1):49–65.

60. Wu X, Li Y, Crise B, Burgess SM. Transcription start regions in the human genome are favored targets for MLV integration. *Science*. 2003;300(5626):1749–1751.

61. Suzuki J, Fujita J, Taniguchi S, Sugimoto K, Mori KJ. Characterization of murine hemopoietic-supportive (MS-1 and MS-5) and non-supportive (MS-K) cell lines. *Leukemia*. 1992;6(5):452–458.

62. Cooper AR, Patel S, Senadheera S, Plath K, Kohn DB, Hollis RP. Highly efficient large-scale lentiviral vector concentration by tandem tangential flow filtration. *J Virol Methods*. 2011;177(1):1–9.

63. Paruzynski A, et al. Genome-wide high-throughput integrome analyses by nrLAM-PCR and next-generation sequencing. *Nat Protoc*. 2010;5(8):1379–1395.

64. Langmead B, Trapnell C, Pop M, Salzberg SL. Ultrafast and memory-efficient alignment of short DNA sequences to the human genome. *Genome Biol*. 2009;10(3):R25.

65. Tukey JW. Variances of variance components: II. The unbalanced single classification. *Ann Math Statist*. 1957;28(1):43–56.

66. Snedecor GW, Cochran WG. *Statistical Methods*. 7th ed. Ames, Iowa, USA: Iowa State University Press; 1989.

67. Lehmann EL, D'Abrera HJM. *Nonparametrics: Statistical Methods Based on Ranks*. New York, New York, USA: Springer; 2006.

68. Fisher RA. On the interpretation of χ2 from contingency tables, and the calculation of P. *J R Stat Soc*. 1922;85(1):87–94.

69. SAS Institute. *SAS/STAT 9.3 User's Guide:: The REG Procedure (Chapter)*. Carey, North Carolina, USA: SAS Institute, Inc.; 2011.